Research of Styrene-Butadiene Rubber/Silicon-Aluminum Oxides Nanotube Binary Nanocomposites

Qingguo Wang,[1] Wenxiu Gao,[1] Liqun Zhang[2]

[1]*Key Laboratory of Rubber-plastics of Ministry of Education, Qingdao University of Science and Technology, Qingdao 266042, China*
[2]*Key Laboratory of Beijing City on Preparation and Processing of Novel Polymer Materials, Beijing University of Chemical Technology, Beijing 100029, China*

Received 10 August 2009; accepted 13 August 2010
DOI 10.1002/app.33245
Published online 11 February 2011 in Wiley Online Library (wileyonlinelibrary.com).

ABSTRACT: A novel silicon-aluminum oxides (Si-Al) nanotubes with length ranging from 500 to 1000 nm were introduced to fabricate the styrene-butadiene rubber (SBR)/Si-Al nanotube binary nanocomposites. Scanning electron microscope observation showed the Si-Al nanotubes up to 20 parts per hundred parts of rubber (phr) loading level were dispersed well in SBR matrix. Mechanical properties tests, thermogravimetry analysis and dynamic mechanical thermal analysis revealed that the Si-Al nanotubes have the effects on improving shore A hardness, tensile strength, tear strength, initial decomposition temperature, and storage modulus while lower the maximum loss factor (tan δ) of the SBR/Si-Al nanotube binary nanocomposites. FTIR spectra analysis showed that new Si—O bond was generated between the hydroxyl group of Si-Al nanotube and the coupling reagent Si69. © 2011 Wiley Periodicals, Inc. J Appl Polym Sci 120: 3196–3203, 2011

Key words: modification; nanocomposites; rubber

INTRODUCTION

Rubber nanocomposites, rubbers modified with nanoscale inorganic fillers, have attracted a great deal of interest because of their superior properties.[1–6] The extent of property improvement depends on the size, the aspect ratio, the degree of dispersion, and orientation of the fillers in the rubber matrix, as well as the degree of adhesion of the fillers to the polymer chains.[7,8] Recently, nanoparticles with various morphologies, including platelets such as layered silicates,[4,9–16] spherical particles such as silica,[5,17–19] carbon nanotubes,[3,20–23] etc.,[6,24–28] have been used as reinforcing fillers in rubbers. Noteworthy, the carbon nanotubes, including the multiwall and the singlewall carbon nanotubes, have attracted enormous attention because of their unique nanotube structural characteristics and their electrical and mechanical properties.[29–31]

In this article, we introduced a novel kind of nanoscale inorganic filler (see Fig. 1), silicon-aluminum oxides (Si-Al) nanotubes with length ranging from 500 to 1000 nm, inner diameter ranging from 10 to 20 nm, and outer diameter ranging from 40 to 60 nm. Containing silicon oxides (58.15%), aluminum oxides (22.21%), water (17.11%), etc., the Si-Al nanotubes having similar tubal structure to abovementioned carbon nanotubes have good thermal stability and high modulus.[32,33] Using the novel Si-Al nanotubes, we prepared the styrene-butadiene rubber (SBR)/Si-Al nanotube binary composites and investigated the dispersion of Si-Al nanotubes in SBR matrix. At the same time, we also studied the effects of Si-Al nanotubes on reinforcement, thermal stability and dynamic mechanical thermal properties of the SBR/Si-Al nanotube binary nanocomposites.

EXPERIMENTAL

Materials

Styrene butadiene rubber (SBR-1502, the M_n is about 100,000, and the molecular weight distribution is about 4–6) manufactured by Qilu rubber Co. Ltd. were used in this study, in which the styrene fraction is 23.5%, the *trans* 1,4-structure and the *cis* 1,4-

Correspondence to: Q. Wang (cnqingguo@yahoo.com).
Contract grant sponsor: Natural Science Foundation of China; contract grant number: 50873049.
Contract grant sponsor: National High Technology Research and Development Program of China (863 Program); contract grant number: 2009AA03Z338.
Contract grant sponsor: Shandong Young Scientists Encouragement Foundation; contract grant number: 2007BS04038.
Contract grant sponsor: Scientific Research Foundation of Shandong Education Department; contract grant number: J07YA12.
Contract grant sponsor: Doctor's Foundation of Qingdao University of Science and Technology.

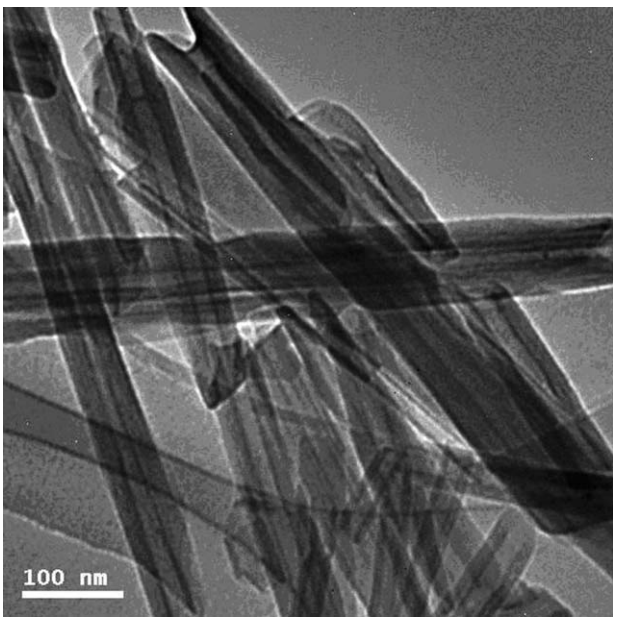

Figure 1 TEM image of the Si-Al nanotubes. (Photo provided by Chinese Zhengzhou Jinyangguang ceramic Co. Ltd)

structure contents of butadiene are 55% and 9.5%, respectively, the 1,2-structure content of butadiene is 12%. Si-Al nanotubes were kindly provided by Zhengzhou Jinyangguang ceramic Co. Ltd. Bis(triethoxysilylpropyl)tetrasulfide (Si69), coupling reagents, was made by Changzhou Oushi rubber aids corp. in China. Zinc oxide (ZnO) with purity of 99.7% was prepared by Zhucheng Xiangtai zinc oxide company in China. Sulfur, vulcanizing accelerate reagent (CZ, *N*-cyclohexyl-2-benzothiazolesulphenamide) and stearic acid (Hst) were purchased from chemical suppliers located in China.

Experimental instruments

The oscillating disc rheometer, GT-M2000-A, was manufactured by Taiwan Gotech Testing Machine Inc. The FTIR spectra were recorded in the 4000–650 cm^{-1} range on a FTIR instrument (VERTEX70, made by Bruker Co. Ltd.); resolution 4 cm^{-1}; interval 0.2. The environmental SEM, JSM-6700, was made by JEOL Corp. of Japan. The thermogravimetry, TGA 209/cell, was made by NETZCH Corp. in Germany. The DMTA, NETZSCH DMA 242, was manufactured by NETZSCH Corp. in Germany. The two-roll mill, SK-160B type, was produced by Shanghai Shuangyi Rubber-Plastics machine Inc. of China. The plate vulcanizing press, XL-40 type, was produced by Shanghai rubber machine Inc. of China.

Preparation of SBR/Si-Al nanotube binary nanocomposites

Table I lists the formulations of the SBR/Si-Al nanotube binary nanocomposites studied in this article. To prepare the nanocomposites, the two rolls of a two-roll mill were adjusted to an adaptive distance at which bulk SBR became fluidic at 60°C. Si-Al nanotubes, Si69, mixture of ZnO, CZ, and Hst were added into the fluidic bulk SBR step by step and mixed for 10 min. Sulfur was then added to the mixture of SBR, Si-Al nanotubos, Si69, ZnO, CZ, and Hst. The final mixture was mixed for approximately 3 min until the sulfur was dispersed well in the SBR matrix. Finally, the SBR compound were sliced into sheets (the thickness is about 2 mm) from the two-roll mill, the following vulcanizing process was performed on a plate vulcanizing press with 25 ton pressure at 150°C to obtain the $120 \times 85 \times 2$ mm^3 rectangular sheets. The cure time for each SBR compound was measured using an oscillating disk rheometer.

Measurement and characterization

Tensile test, tear strength, and shore A hardness of the SBR/Si-Al nanotube binary nanocomposites were measured according to GB/T528-1998, GB/T529-1999, and GB/T531-1999, respectively. The speed of tensile and tear tests was 500 mm/min at room temperature. The curing characteristics of neat SBR and SBR/Si-Al nanotube binary nanocomposites were assessed at 150°C using an oscillating disc rheometer.

The fracture surfaces of SBR/Si-Al nanotube binary nanocomposites prepared for the SEM image observation were obtained at the liquid nitrogen temperature and were sputter-coated with a thin gold layer before observation. TGA of neat SBR and SBR/Si-Al nanotube binary nanocomposites samples (about 10 mg) were performed in N_2 atmosphere (flow rate: 50 mL/min) at temperatures ranging from 30 to 650°C with a heat rising rate of 10°C/min. The dynamic mechanical thermal analyzer (DMTA) was performed on the dual cantilever bend mode with the frequency of 10 Hz in the temperature range from −80 to 100°C with an elevation rate of 3°C/min.

TABLE I
Formulations of Various SBR/Si-Al Nanotube Binary Nanocomposites

SBR (phr)	Si-Al nanotube (phr)	Si69 (phr)	S (phr)	ZnO (phr)	CZ[a] (phr)	Hst[b] (phr)
100	0	0	1.75	3	1	1
100	1	0.1	1.75	3	1	1
100	3	0.3	1.75	3	1	1
100	5	0.5	1.75	3	1	1
100	10	1.0	1.75	3	1	1
100	20	2.0	1.75	3	1	1

All the ingredients are in parts per hundred parts of rubber (phr).
[a] *N*-cyclohexyl-2-benzothiazolesulphenamide.
[b] Stearic acid.

RESULTS AND DISCUSSION

Morphology of SBR/Si-Al nanotube binary nanocomposites

Figure 2 illustrates the SEM images of fracture surfaces of SBR/Si-Al nanotube binary nanocomposites comprising 3, 5, 10, and 20 phr Si-Al nanotube loadings, respectively. It can be seen that the Si-Al nanotubes up to 20 phr loading level were dispersed well in the SBR matrix without obvious agglomerates, and the SEM images with 30,000 magnification level demonstrated distinct tubal shape of the nanotubes. As we expected, with the Si-Al nanotube loading level increasing, the distances between the Si-Al nanotubes in SBR matrix became shorter.

Generally, untreated nanoscale inorganic fillers are not easily dispersed well in polymer matrix because of their smaller particle sizes and stronger adsorption.[1,9,34,35] Our study, however, showed that Si-Al nanotubes up to 20 phr loading were dispersed well in the SBR matrix. It can be explained as the tubal Si-Al nanoparticles (length: 500–1000 nm; inner diameter: 10–20 nm; outer diameter: 40–60 nm) had lower tendency of agglomerating because of their relatively smaller interface and weaker interactions among the Si-Al nanotubes. On the other hand, the adding of coupling reagent Si69 also is beneficial to the compatibility between the Si-Al nanotubes and the SBR, leading to good dispersion of Si-Al nanotubes in the SBR matrix. The good dispersion of the Si-Al nanotubes in the SBR matrix may endow the SBR/Si-Al nanotube binary nanocomposites with enhanced mechanical properties, thermal stability, and dynamic thermal mechanical properties.

Mechanical properties of SBR/Si-Al nanotube binary nanocomposites

Figure 3 illustrates the mechanical properties of neat SBR and SBR/Si-Al nanotube binary nanocomposites. As shown in Figure 3(A), with the Si-Al nanotube loading level increasing, the elongation at break and the tensile strength of the SBR/Si-Al nanotube binary nanocomposites increased. Compared with neat SBR, 1 phr Si-Al nanotubes loading in SBR matrix leads to a 42% increase in elongation at break and a 10% increase in tensile strength, while 3 phr Si-Al nanotubes loading leading to 68% increase in elongation at break and 36% increase in tensile strength. These results clearly showed that the Si-Al nanotubes have good effects on improving the mechanical properties of SBR composites.

Figure 3(B) shows the stresses of SBR/Si-Al nanotube binary nanocomposites in 100 and 300% strains, respectively. Figure 3(C) shows the tear strength and hardness of SBR/Si-Al nanotube binary nanocomposites. It is observed that the stresses in 100 and 300% strains, tear strength, and shore A hardness of the SBR binary nanocomposites increased along with the Si-Al nanotubes loading increasing, and the hardness of SBR binary nanocomposites has the similar changing tendency with its tensile strength along with the Si-Al nanotube loading increasing.

Based on above results, we speculate there are some interaction existed between the SBR matrix and the Si-Al nanotube, and the Si-Al nanotube loading facilitates the formation of interaction, thus leading to the mechanical properties of SBR/Si-Al nanotuble composites increasing. Generally, there are two kinds of interaction between polymer matrix and filler surface, the physical absorption and the chemical interaction. When the Si-Al nanotubes were dispersed well in SBR matrix, there are much interface between the filler and the rubber matrix. The Si-Al nanotubes acted as the physical links in polymer matrix and induce the formation of "entangled structure" that hinder the mobility of rubber chains.[36] With the Si-Al nanotubes increasing, both the amount of physical links and interface between SBR matrix and Si-Al nanotubes increased, indicating greater interaction between the SBR matrix and the Si-Al nanotubes. Therefore, the tensile strength and tear strength of the SBR/Si-Al nanotube binary nanocomposites improved during stretching process, while the increased stiffness of the SBR/Si-Al nanotube binary nanocomposites may be explained as that the Si-Al nanotubes have the effect on restricting the motion of SBR macromolecules.

As well known, the coupling reagent Si69 can react with the hydroxyl group of silica while the Si69 reacts with the rubber chains with the sulfur bridge, thus improving the chemical interaction between the rubber matrix and silica.[37] In this article, some chemical interactions maybe happen between the Si-Al nanotube and rubber matrix. To explain the effect of the reagent Si69 on the chemical interaction formation between SBR macromolecules and Si-Al nanotubes, we also fabricated the comparable SBR/Si-Al nanotube binary composites containing 20 phr Si-Al nanotube loading without the Si69. Experimental results showed that the tensile strength and tear strength of the SBR/Si-Al nanotube binary composites without Si69 is 3.3 MPa and 12.2 k*N*/m respectively, which are inferior to those of the SBR/Si-Al nanotube binary composites with Si69, explaining that the reagent Si69 has reacted in the SBR/Si-Al composites and plays an important role in the reinforcement of the SBR/Si-Al binary nonocomposites.

FTIR analysis of the coupling mechanism in SBR/Si-Al nanotube nanocomposites

Figure 4 is the FTIR spectra of Si-Al nanotube, neat SBR, and various SBR/Si-Al nanotube composites. The peak areas at 3696 and 3623 cm^{-1} are associated

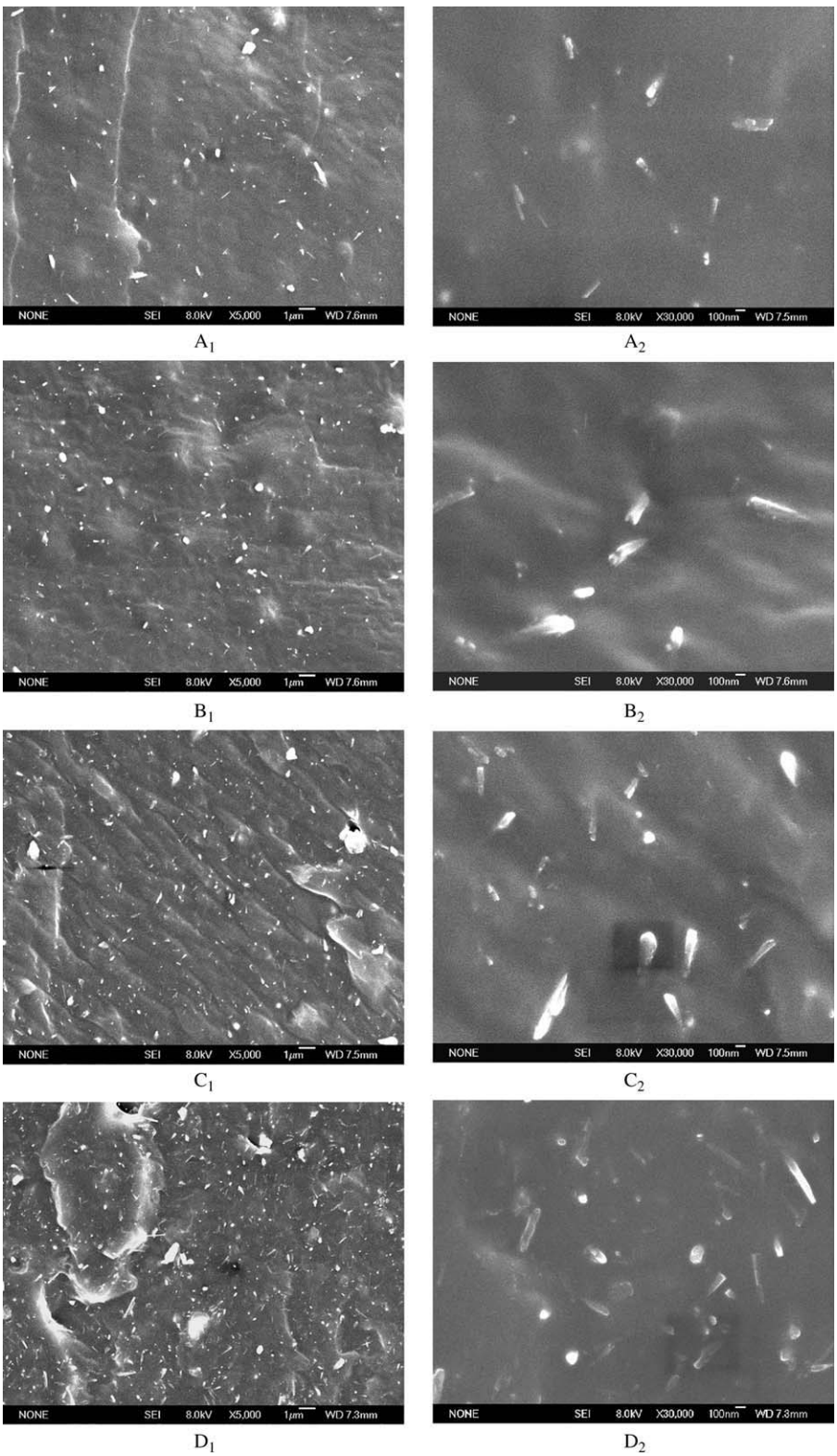

Figure 2 SEM images of fracture surfaces of SBR/Si-Al nanotube binary nanocomposites filled with different Si-Al nanotube loadings. A: 3 phr Si-Al nanotubes; (B) 5 phr Si-Al nanotubes; (C) 10 phr Si-Al nanotubes; (D) 20 phr Si-Al nanotubes. Subscript 1 represents the magnification of 5000 and subscript 2 represents the magnification of 30,000.

with the stretching vibration of —OH group of Si-Al nanotube, which make it possible that the new Si—O bond is generated between Si69 and —OH group of Si-Al nanotube.[37]

In this article, we elected the spectra band of methyl (2840 cm^{-1}), methylene (2920 cm^{-1}), and *trans*-1,4-butadiene (964 cm^{-1}) as the comparable internal standards. Though the concentration of

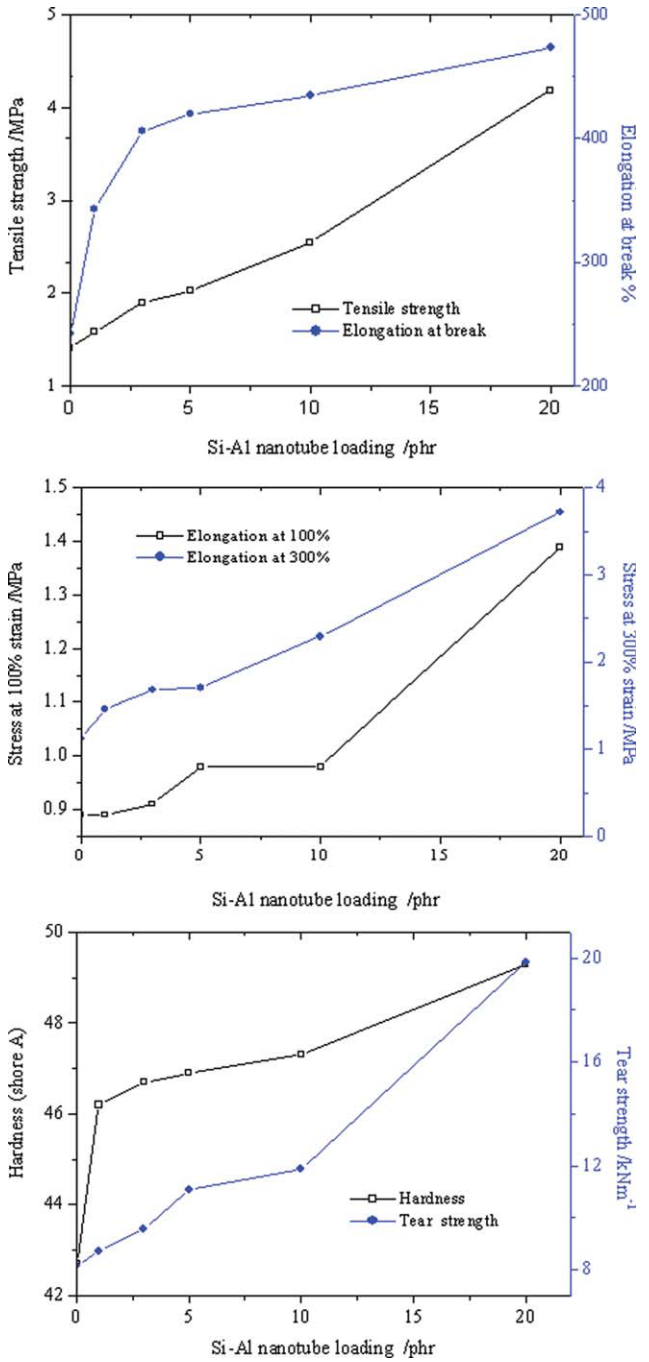

Figure 3 Mechanical properties of SBR/Si-Al nanotube binary nanocomposites versus Si-Al nanotube loadings. [Color figure can be viewed in the online issue, which is available at wileyonlinelibrary.com.]

methyl, methylene, and *trans*-1,4-butadiene of SBR/Si-Al nanotube composites decrease with the Si-Al nanotube loading level increasing, the corresponding decrease degrees are in agreement with their absorption intensity changing in general.

Compared with the FTIR spectrum of Si-Al nanotube, the FTIR spectra of SBR/Si-Al nanotube composites have a new absorption band at 1083 cm^{-1}, which can be assigned to stretch vibration of the Si—O bond[38] generated between Si-Al nanotube and coupling reagents Si69. At the same time, the coupling reagent Si69 also reacted with the rubber chains by forming mono-, di-, and polysulfidic covalent bonds.[37] With the Si-Al nanotube loading level increasing, the absorption intensity at 1083 cm^{-1} increases, indicating more Si—O bond was generated in the SBR/Si-Al nanotube composites, which leads to higher interaction between the Si-Al nanotubes and SBR matrix and higher reinforcement of the SBR/Si-Al nanotube binary nanocomposites.

Thermal stability of SBR/Si-Al nanotube binary nanocomposites

Figure 5 illustrates the thermogravimetry analysis of neat SBR and SBR/Si-Al nanotube binary nanocomposites decomposed in N_2. Figure 5(A) shows two decomposition stages in temperature range from 150 to 550°C for both neat SBR and SBR/Si-Al nanotube binary nanocomposites. The weight loss rates (decomposition rate) of neat SBR and SBR/Si-Al nanotube binary nanocomposites during the first decomposition stage (temperature ranging from 150 to 300°C) appeared to be slower than those in the second decomposition stage [temperature ranging from 300 to 550°C, see Fig. 5(B)]. Compared with neat SBR, the SBR/Si-Al nanotube binary nanocomposites, however, showed slightly faster weight loss rates at the first decomposition stage and the weight loss rate of the SBR binary nanocomposites containing 20 phr Si-Al nanotubes loading was slightly faster than that of the SBR binary nanocomposites containing 10 phr Si-Al nanotubes. The maximum weight loss rate (corresponding to the peak of DTG

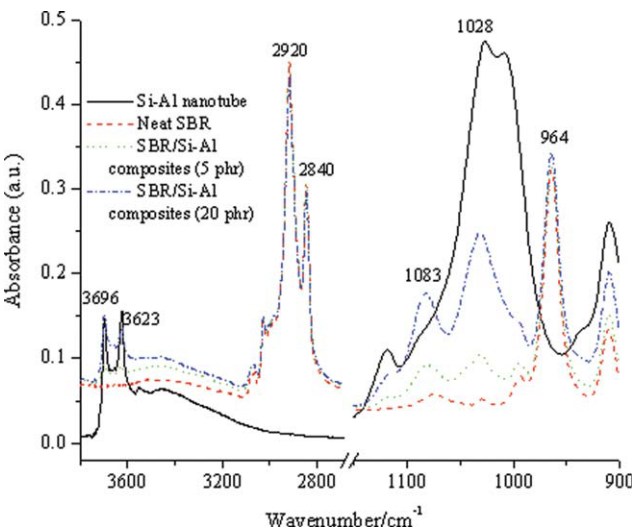

Figure 4 FTIR spectra of Si-Al nanotube, neat SBR and various SBR/Si-Al nanotube binary nanocomposites. [Color figure can be viewed in the online issue, which is available at wileyonlinelibrary.com.]

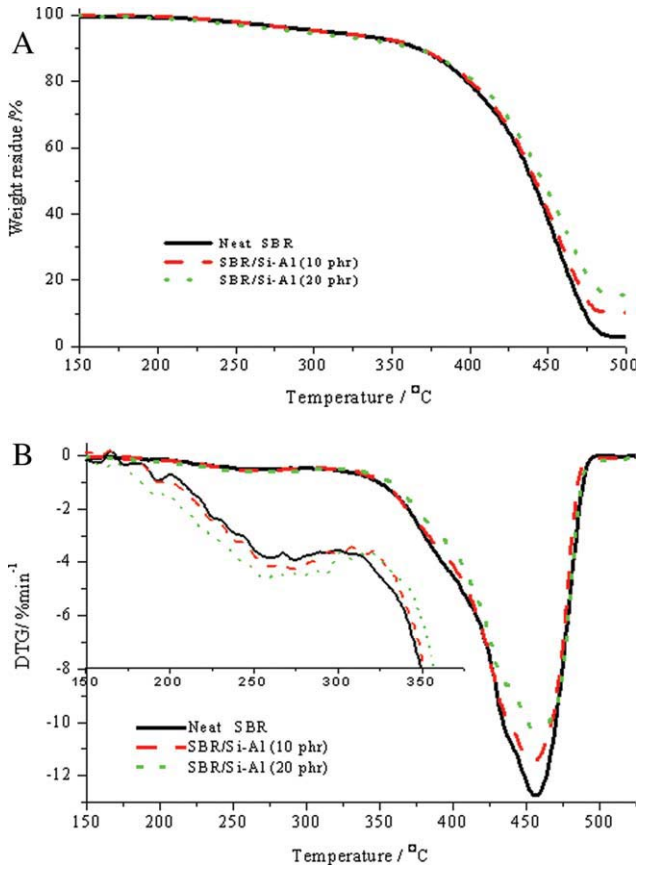

Figure 5 Thermogravimetry analysis curves of neat SBR and SBR/Si-Al nanotube binary nanocomposites. A: weight residue curves of SBR composites versus temperature; (B) DTG curves of SBR composites versus temperature. [Color figure can be viewed in the online issue, which is available at wileyonlinelibrary.com.]

curve) of neat SBR at the first decomposition stage happened in the mass change of 5.16% (corresponding to the temperature of 274.3°C) whereas those of two SBR/Si-Al nanotube binary nanocomposites happened in the mass changes of 5.29% and 6.16% (corresponding to the temperatures of 273.5°C and 256.9°C), respectively. As Grieco et al.[39] reported that the first decomposition stage corresponds to the decomposition of some compounds added to the SBR, and the temperature corresponding to the beginning of SBR weight loss is higher than 350°C, which was observed in the second decomposition stage in our study. Although the differences among the decomposition rates of neat SBR and SBR/Si-Al nanotube binary nanocomposites with different Si-Al nanotubes loadings are minimal, the results seem to indicate that the Si-Al nanotubes were able to accelerate the decomposition rate of the SBR composites in the first decomposition stage.

As shown in Figure 5(B), the influence of Si-Al nanotubes to the decomposition rate of the SBR at the second decomposition stage was totally different from that of the first decomposition stage. At the second decomposition stage, the decomposition rate of neat SBR was faster than those of SBR binary nanocomposites, and the weight loss rate of the SBR binary nanocomposite containing 10 phr Si-Al nanotubes was higher than that of the SBR binary nanocomposite containing 20 phr Si-Al nanotubes. This result indicates that the Si-Al nanotubes might be able to slightly slow down the decomposition rate and improve the thermal stability of SBR composites at higher temperatures.

As we explained earlier, with the Si-Al nanotubes loadings increasing, more Si-Al nanotubes, which have better thermal stability than SBR does at high temperatures, were adhered to the SBR macromolecules, leading to larger interface between SBR macromolecules and the Si-Al nanotubes. Therefore, in SBR/Si-Al nanotube binary nanocomposites, the Si-Al nanotubes may have played an important role in retarding the decomposition of SBR macromolecules by acting as insulators and mass transport barriers against the heat transition and the volatility of pyrolysis products. And this may be the reason why the SBR/Si-Al nanotube binary nanocomposites showed slightly better thermal stability (higher initial temperature of SBR macromolecular decomposition) than neat SBR did in our study, while the SBR/Si-Al nanotube binary nanocomposites containing 20 phr Si-Al nanotubes has better thermal stability than those containing 10 phr Si-Al nanotubes. However, further studies are needed to obtain an affirmative conclusion.

Dynamic mechanical thermal analysis of SBR/Si-Al nanotube binary nanocomposites

Figure 6(A) shows the temperature dependence of loss factor (tan δ) and storage modulus (E') of the samples. The maximum tan δ values of various SBR composites were different. With the Si-Al nanotube loading increasing, the maximum tan δs of the corresponding SBR/Si-Al nanocomposites decreases. The maximum tan δ of neat SBR was 1.53 whereas those of the SBR/Si-Al nanotube binary nanocomposites containing 10 phr and 20 phr Si-Al nanotube were 1.48 and 1.40, respectively. With the Si-Al nanotubes loading increasing, the mobility of the SBR macromolecules became more difficult because of the restraint induced by the Si-Al nanotubes, thus lower tan δ values of the SBR/Si-Al nanotube binary nanocomposites were obtained.

It is widely accepted that the temperature corresponding to the peak of tan δ curve is considered as the glass transition temperature (T_g) of the polymer, and the T_g value of polymer nanocomposites containing nanoscale inorganic filler increases with the inorganic fillers increasing.[40,41] In our study, the neat SBR and the SBR/Si-Al nanotube binary nanocomposites, however, demonstrated the comparable T_g (about −19°C) values.

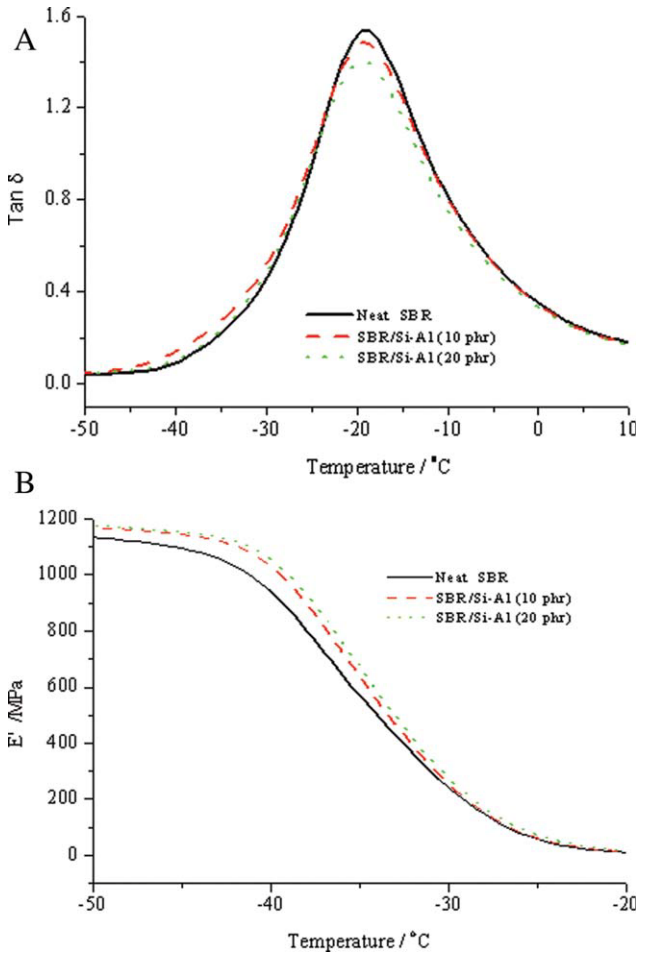

Figure 6 Dynamic mechanical thermal analysis of neat SBR and SBR/Si-Al nanotube binary nanocomposites. [Color figure can be viewed in the online issue, which is available at wileyonlinelibrary.com.]

Figure 6(B) shows the storage modulus (E') of SBR/Si-Al nanotube binary composites increases with the Si-Al nanotubes loading increasing. The higher E' value of the SBR/Si-Al composites was probably induced by both of the Si-Al nanotubes' high modulus and the Si-Al nanotubes' restricting on the motion of segments of SBR macromolecular chains. With the loading of Si-Al nanotubes increasing, the motion of SBR macromolecules chains became more difficult, and that's why the corresponding storage modulus of the SBR nanocomposites containing higher Si-Al nanotubes were higher than those of the SBR nanocomposites containing less Si-Al nanotubes.

In our study, although the Si-Al nanotubes were well dispersed in SBR matrix, the mechanical properties, thermal stability, and dynamic thermomechanical properties of the SBR/Si-Al nanotube binary nanocomposites were not improved dramatically as we expected. One possible reason is that the tubal shape and lengths of the Si-Al nanotubes were changed during the mixing process, which weakens its capability of improving the SBR nanocomposites's properties. The other possible reason is that there was not enough interaction generated between the Si-Al nanotubes and the SBR matrix.

CONCLUSIONS

Using the novel Si-Al oxide nanotubes, we have fabricated some SBR/Si-Al nanotube binary nanocomposites. Experiment showed that the Si-Al nanotubes up to 20 phr loading can be dispersed well in SBR matrix and can moderately improve the hardness, tensile strength, tear strength, initial decomposition temperature, and storage modulus of the SBR/Si-Al nanotube binary nanocomposites, in which a new Si—O bond was generated between the Si-Al nanotube and the coupling reagent Si69.

References

1. Bhattacharya, M.; Maiti, M.; Anil K. Polym Eng Sci 2009, 49, 81.
2. Pradhan, S.; Costa, F. R.; Wagenknecht, U.; Jehnichen, D.; Bhowmick, A. K.; Heinrich, G. Eur Polym J 2008, 44, 3122.
3. Endo, M.; Noguchi, T.; Ito, M.; Takeuchi, K.; Hayashi, T.; Kim, Y. A.; Wanibuchi, T.; Jinnai, H.; Terrones, M.; Dresselhaus, M. S. Adv Funct Mater 2008, 18, 3403.
4. Acharya, H.; Kuila, T.; Srivastava, S. K.; Bhowmick, A. K. Polym Compos 2008, 29, 443.
5. Chen, Y.; Peng, Z.; Kong, L. X.; Huang, M. F.; Li, P. W. Polym Eng Sci 2008, 48, 1674.
6. Ismail, H.; Pasbakhsh, P.; Fauzi, M. N. A.; Abu Bakar, A. Polym Test 2008, 27, 841.
7. Bokobza, L. Polymer 2007, 48, 4907.
8. Bokobza, L. Macromol Mater Eng 2004, 289, 607.
9. Arroyo, M.; López-Manchado, M. A.; Herrero, B. Polymer 2003, 44, 2447.
10. Kato, M.; Tsukigase, A.; Tanaka, H.; Usuki, A.; Inai, I. J Polym Sci Part A: Polym Chem 2006, 44, 1182.
11. Maiti, M.; Bhowmick, A. K. Polymer 2006, 47, 6156.
12. Liang, Y. R.; Lu, Y. L.; Wu, Y. P.; Ma, Y.; Zhang, L. Q. Macromol Rapid Commun 2005, 26, 926.
13. Psarras, G. C.; Gatos, K. G.; Karger-Kocsis, J. J Appl Polym Sci 2007, 106, 1405.
14. Song, M.; Wong, C. W.; Jin, J.; Ansarifar, A.; Zhang, Z. Y.; Richardson, M. Polym Int 2005, 54, 560.
15. Valadares, L. F.; Leite, C. A. P.; Galembeck, F. Polymer 2006, 47, 672.
16. Takahashi, S.; Goldberg, H. A.; Feeney, C. A.; Karim, D. P.; Farrell, M.; O'Leary, K.; Paul, D. R. Polymer 2006, 47, 3083.
17. Zeng, M.; Sun, X.; Yao, X.; Ji, G.; Chen, N.; Wang, B.; Qi, C. J Appl Polym Sci 2007, 106, 1347.
18. Peng, Z.; Kong, L. X.; Li, S.-D.; Chen, Y.; Huang, M. F. Compos Sci Technol 2007, 67, 3130.
19. Liu, X.; Zhao, S. J Appl Polym Sci 2008, 109, 3900.
20. Valentini, L.; Biagiotti, J.; Kenny, J. M.; López Manchado, M. A. J Appl Polym Sci 2003, 89, 2657.
21. De Falco, A.; Goyanes, S.; Rubiolo, G. H.; Mondragon, I.; Marzocca, A. Appl Surf Sci 2007, 254, 262.
22. Bokobza, L.; Rahmani, M.; Belin, C.; Bruneel, J.-L. J Polym Sci Part B: Polym Phys 2008, 46, 1939.
23. Sui, G.; Zhong, W. H.; Yang, X. P.; Yu, Y. H.; Zhao, S. H. Polym Adv Technol 2008, 19, 1543.
24. Ismail, H.; Pasbakhsh, P.; Fauzi, M. N. A.; Abu Bakar, A. Polym Test 2008, 27, 841.

25. Wang, Y.; Zhang, H.; Wu, Y.; Yang, J.; Zhang, L. Eur Polym J 2005, 41, 2776.
26. Tian, M.; Cheng, L.; Liang, W.; Zhang, L. Macromol Mater Eng 2005, 290, 681.
27. Chen, L.; Chen, G. H.; Lu, L. Adv Funct Mater 2007, 17, 898.
28. Scott Parent, J.; Liskova, A.; Resendes, R. Polymer 2004, 45, 8091.
29. Iijima, S. Nature 1991, 354, 56.
30. Barraza, H. J.; Pompeo, F.; O'Rear, E. A.; Resasco, D. E. Nano Lett 2002, 2, 797.
31. Frogley, M. D.; Ravich, D.; Wagner, H. D. Compos Sci Technol 2003, 63, 1647.
32. Cheng, Z.; Ma, B. Chin J Funct Mater 2007, 38 (A06), 2320.
33. Ma, B.; Cheng, Z.; Kong, L. China Pat. 200,710,189,888.8 (2007).
34. Shih, Y. F.; Chen, L. S.; Jeng, R. J. Polymer 2008, 49, 4602.
35. Shin, Y.; Lee, D.; Lee, K.; Ahn, K. H.; Kim, B. J Ind Eng Chem 2008, 14, 515.
36. López-Manchado, M. A.; Valentín, J. L.; Carretero, J.; Barroso, F.; Arroyo, M. Eur Polym J 2007, 43, 4143.
37. ten Brinke, J. W.; Debnath, S. C.; Reuvekamp, L. A. E. M.; Noordermeer, J. W. M. Compos Sci Technol 2003, 63, 1165.
38. Lenza, R. F. S.; Vasconcelos, W. L. Mater Res 2001, 4, 175.
39. Grieco, E.; Bernardi, M.; Baldi, V. J Anal Appl Pyrolysis 2008, 82, 304.
40. Meneghetti, P.; Qutubuddin, S. Thermochim Acta 2006, 442, 74.
41. Kim, S. H.; Chung, J. W.; Kang, T. J.; Kwak, S.-Y.; Suzuki, T. Polymer 2007, 48, 4271.